

## Stability of Hagen–Poiseuille flow with superimposed rigid rotation

By P.-A. MACKRODT

Institut für Strömungsmechanik der Deutschen Forschungs- und  
Versuchsanstalt für Luft- und Raumfahrt E.V.,  
Aerodynamische Versuchsanstalt, Göttingen, Germany

(Received 10 May 1974 and in revised form 23 June 1975)

The linear stability of Hagen–Poiseuille flow (Poiseuille pipe flow) with superimposed rigid rotation against small three-dimensional disturbances is examined at finite and infinite axial Reynolds numbers. The neutral curve, which is obtained by numerical solution of the system of perturbation equations (derived from the Navier–Stokes equations), has been confirmed for finite axial Reynolds numbers by a few simple experiments. The results suggest that, at high axial Reynolds numbers, the amount of rotation required for destabilization could be small enough to have escaped notice in experiments on the transition to turbulence in (nominally) non-rotating pipe flow.

---

### 1. Introduction

In his historic experiments Reynolds (1883) found that the onset of turbulence in pipe flow depends only on the ratio  $W_0 R/\nu$  (where  $W_0$  is the maximum velocity,  $R$  the radius of the pipe and  $\nu$  the kinematic viscosity), which we now call the Reynolds number  $Re$ . He found that in his experimental set-up the critical Reynolds number was about 13 000. But Reynolds did not succeed in an attempt (1895) to predict this value theoretically. Theoretical work in this field started again with Sexl (1927*a, b*), who found no evidence of instability of Hagen–Poiseuille flow (HPF) to small *two-dimensional* (axisymmetric) disturbances. His results were supported and extended to infinite Reynolds number by many other authors, e.g. Mott & Joseph (1968), Davey & Drazin (1969) and Crowder & Dalton (1971). Subsequently the stability of Poiseuille pipe flow to small *three-dimensional* disturbances was examined too. Lessen, Sadler & Liu (1968) found no amplification of such disturbances up to a Reynolds number of 16 000, by numerical solution of the perturbation equations. Salwen & Grosch (1972) confirmed the results of Lessen *et al.* and extended the calculations up to a Reynolds number of 50 000. The most recent work on this subject (Gill 1973) made it clear that even the least damped perturbation mode has a finite decay rate for any Reynolds number, however large.

Thus, from the theoretical point of view, HPF appears to be stable against all kinds of infinitesimal perturbations at all Reynolds numbers, whereas in many experiments spontaneous transition from laminar to turbulent pipe flow has been observed at Reynolds numbers between 2300 and nearly 50 000 (see, for example,

Reshotko 1958; Bhat 1966). The usual interpretation is that HPF is stable against infinitesimal disturbances but unstable to perturbations of finite amplitude (Leite 1959). Considering the extremely sophisticated experimental set-ups used by investigators, the most likely sources of perturbations which could have influenced the flow are disturbances to the fluid in the feeding tank. This assumption is strongly supported by the results of Schiller (1922), who stated that the critical Reynolds number increases as the time for which the fluid is allowed to settle in the feeding tank increases. However the motion in the feeding tank which remains after a long settling time can be only a very slow rotation, thus superimposing an azimuthal velocity  $V$  upon the Hagen–Poiseuille flow. Furthermore, from the results of Ludwig (1960, 1961, 1964), Kiessling (1963), Mackrodt (1967) and Wedemeyer (1967, 1969) it is well known that a slight rotation superimposed on the axial velocity destabilizes the flow in a cylindrical annulus. Pedley (1968, 1969) and Joseph & Carmi (1969) found independently that a very rapidly rotating flow in a pipe becomes unstable at  $Re = 82.9$ . These results have been confirmed experimentally by Nagib *et al.* (1971) and theoretically by Strohl (1969), Hung, Joseph & Munson (1972), and Metcalfe & Orszag (1973).

These findings suggest that *linear* rather than finite amplitude instability, associated with an undetected, slow rotation superimposed on HPF, could be responsible for its apparent spontaneous transition. Actually this remaining rotation cannot be rigid, both because of friction near the tube wall and, more important, because of the radial variation in vortex stretching that would occur even in an inviscid inlet flow. However there is reason to expect that the qualitative character of the results would persist with more realistic profiles; see the discussion in §4 below.

## 2. Derivation of the perturbation equations

### 2.1. Finite axial Reynolds number

We consider a fully developed laminar flow in a rotating pipe. After a certain inlet length the fluid rotates rigidly with the same angular velocity  $\omega$  as the pipe. The parabolic Poiseuille profile of the axial flow remains uninfluenced. In cylindrical polar co-ordinates  $(r, \phi, z)$  this flow has velocity components  $\{0, \omega r, W_0(1 - r^2/R^2)\}$ , and the pressure is  $\frac{1}{2}\rho\omega^2 r^2$ . Upon the basic flow are superimposed small disturbances  $(\hat{u}, \hat{v}, \hat{w}, \hat{p})$  of the form

$$\hat{u}(r, \phi, z, t) = u(r) \exp[i(\alpha z + \gamma \phi - \beta t)] \quad \text{etc.} \dagger \quad (2.1)$$

The axial wavenumber  $\alpha$  is taken as real, the azimuthal wavenumber  $\gamma$  as an integer, and the frequency  $\beta$  in general as complex; thus we look at disturbances which increase or decrease with time  $t$ . To render all expressions and equations dimensionless the following transformation is introduced:

$$x = r/R, \quad (2.2)$$

† We look at three-dimensional disturbances only, because from the work of Ludwig (1960, 1961) it is well known that in spiral flows, as examined here, such disturbances are more unstable than axisymmetric perturbations.

$$\{\tilde{u}(x), \tilde{v}(x), \tilde{w}(x)\} = (x/W_0) \{u, v, w\}, \quad (2.3)$$

$$\bar{p}(x) = p/\rho W_0^2, \quad (2.4)$$

$$\bar{\alpha} = \alpha R, \quad c = \beta/\alpha W_0, \quad (2.5), (2.6)$$

$$Re_\phi = V_0 R/\nu, \quad Re_z = W_0 R/\nu \quad (2.7), (2.8)$$

( $V_0 = \omega R$  is the azimuthal speed of the pipe wall). The velocity components of the basic flow are now written as  $\{0, V_0 x, W_0(1-x^2)\}$ . After substituting the disturbances (2.1) into the Navier-Stokes equations and the continuity equation and linearizing we obtain a system of four linear, homogeneous, ordinary differential equations, which are written [in the notation of (2.2)–(2.8)] as

$$\tilde{u}'' - \frac{\tilde{u}'}{x} - \tilde{u} \left[ \frac{\gamma^2}{x^2} + \bar{\alpha}^2 + i\bar{\alpha} Re_z(1-x^2-c) + i\gamma Re_\phi \right] - 2\tilde{v} \left( i \frac{\gamma}{x^2} - Re_\phi \right) - Re_z x \bar{p}' = 0, \quad (2.9)$$

$$\tilde{v}'' - \frac{\tilde{v}'}{x} - \tilde{v} \left[ \frac{\gamma^2}{x^2} + \bar{\alpha}^2 + i\bar{\alpha} Re_z(1-x^2-c) + i\gamma Re_\phi \right] + 2\tilde{u} \left( i \frac{\gamma}{x^2} - Re_\phi \right) - i\gamma Re_z \bar{p} = 0, \quad (2.10)$$

$$\tilde{w}'' - \frac{\tilde{w}'}{x} - \tilde{w} \left[ \frac{\gamma^2-1}{x^2} + \bar{\alpha}^2 + i\bar{\alpha} Re_z(1-x^2-c) + i\gamma Re_\phi \right] + 2Re_z x \tilde{u} - i\bar{\alpha} Re_z \bar{p} = 0, \quad (2.11)$$

$$\tilde{u}' + i\gamma \tilde{v}/x + i\bar{\alpha} \tilde{w} = 0 \quad (2.12)$$

(primes denote differentiation with respect to  $x$ ).

The solutions of these differential equations have to satisfy seven boundary conditions. At the wall, these are zero velocity for all three components:

$$\tilde{u}(1) = \tilde{v}(1) = \tilde{w}(1) = 0. \quad (2.13)$$

At the axis of the pipe,  $x = 0$ , the solutions are required to be non-singular: the components  $\hat{u}$  and  $\hat{v}$  have to be free of sources and concentrated vorticity, while the disturbances  $\hat{w}$  and  $\hat{p}$  must be single-valued, which for  $\gamma \neq 0$  is possible only if the amplitude functions  $w$  and  $p$  vanish, and thus

$$\tilde{u}(0) = \tilde{v}(0) = \tilde{w}(0) = \bar{p}(0) = 0 \quad (2.14)$$

[note the factor  $x$  in (2.3)]. The development of the perturbation equations and the formulation of the boundary conditions has been outlined in more detail by the author (1971).

### 2.2. Infinite axial Reynolds numbers

To go to the limit  $Re_z \rightarrow \infty$  in (2.9)–(2.12) one needs further information. From the numerical solutions of this system (see §3.1) it was found that, for large values of  $Re_z$ , the axial wavenumber  $\alpha$  decreases with increasing  $Re_z$  on the stability boundary in such a manner that the product  $\bar{\alpha} Re_z = \tilde{R}$  remains constant (figure 1). That means that the limiting processes  $Re_z \rightarrow \infty$  and  $\bar{\alpha} \rightarrow 0$  must be carried out simultaneously. Furthermore we assume the existence of finite

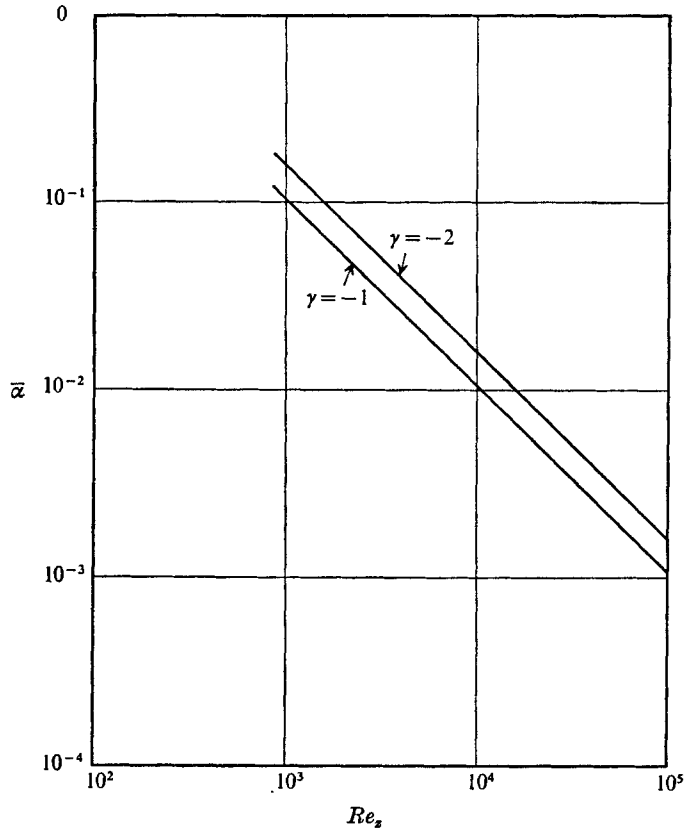


FIGURE 1. Variation of axial wavenumber  $\bar{\alpha}$  with  $Re_x$ .

limiting values  $\tilde{P} = \bar{p}/\bar{\alpha}$  and  $\tilde{W} = \bar{\alpha}\tilde{w}$  for  $Re_x \rightarrow \infty$  with  $\bar{\alpha} \rightarrow 0$ . With these assumptions the perturbation equations (2.9)–(2.12) become

$$\tilde{u}'' - \frac{\tilde{u}'}{x} - \tilde{u} \left[ \frac{\gamma^2}{x^2} + i\tilde{R}(1-x^2-c) + i\gamma Re_\phi \right] - 2\tilde{v} \left( i \frac{\gamma}{x^2} - Re_\phi \right) - \tilde{R}\tilde{P}'x = 0, \quad (2.15)$$

$$\tilde{v}'' - \frac{\tilde{v}'}{x} - \tilde{v} \left[ \frac{\gamma^2}{x^2} + i\tilde{R}(1-x^2-c) + i\gamma Re_\phi \right] + 2\tilde{u} \left( i \frac{\gamma}{x^2} - Re_\phi \right) - i\gamma\tilde{R}\tilde{P} = 0, \quad (2.16)$$

$$\tilde{W}'' - \frac{\tilde{W}'}{x} - \tilde{W} \left[ \frac{\gamma^2 - 1}{x^2} + i\tilde{R}(1-x^2-c) + i\gamma Re_\phi \right] + 2\tilde{u}\tilde{R}x = 0, \quad (2.17)$$

$$\tilde{u}' + i\gamma\tilde{v}/x + i\tilde{W} = 0. \quad (2.18)$$

The boundary conditions (2.13) and (2.14) remain unchanged and are written (using the new variables  $\tilde{P}$  and  $\tilde{W}$ ) as

$$\tilde{u}(1) = \tilde{v}(1) = \tilde{W}(1) = 0 \quad (2.19)$$

and 
$$\tilde{u}(0) = \tilde{v}(0) = \tilde{W}(0) = \tilde{P}(0) = 0. \quad (2.20)$$

A more detailed development of the perturbation equations in the case  $Re_x \rightarrow \infty$  has been given by the author (1973).

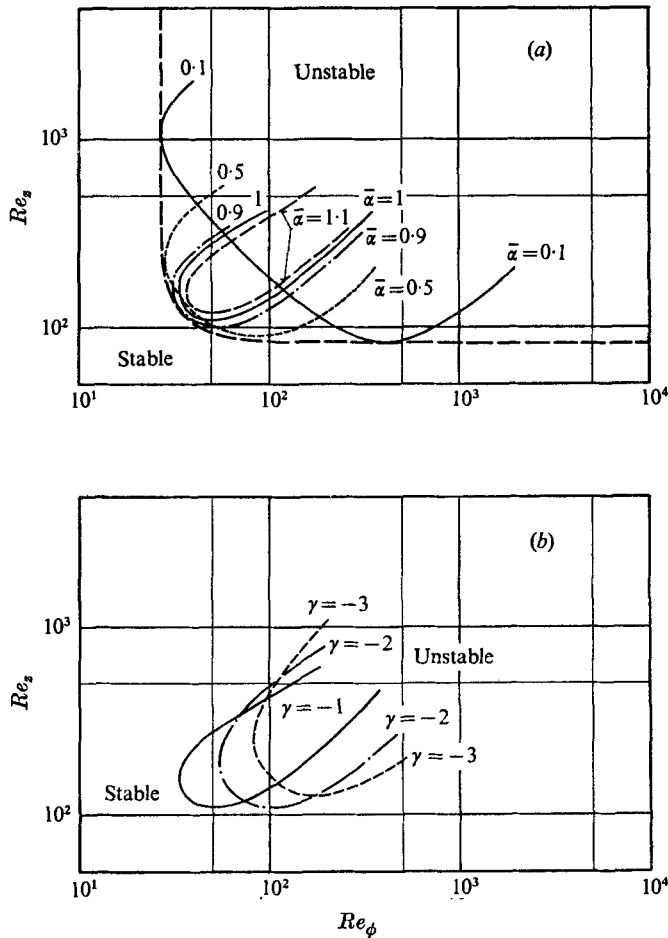


FIGURE 2. Neutral curves for (a) different  $\bar{\alpha}$  at  $\gamma = -1$  (with envelope) and (b) different  $\gamma$  at  $\bar{\alpha} = 1$ .

### 3. Solution of the perturbation equations

#### 3.1. Finite axial Reynolds numbers

The differential equations (2.9)–(2.12) were solved numerically by means of the Runge–Kutta method. To this end the functions  $\tilde{u}$ ,  $\tilde{v}$ ,  $\tilde{w}$  and  $\bar{p}$  were initially represented at  $x = 0$  by expansions in powers of  $x$  which satisfy the boundary conditions at  $x = 0$ . To start the numerical procedure it was further convenient to have an initial approximation to the eigenvalue  $c$ . To this end solutions of the perturbation equations were sought for the limits  $Re_\phi \rightarrow 0$  and  $Re_z \rightarrow 0$  simultaneously. The perturbation equations then took a form for which analytical solutions (expressible in terms of cylinder functions) could be obtained. With these starting values of  $c$  the solutions for finite  $Re_z$  at  $Re_\phi = 0$ , i.e. for Hagen–Poiseuille flow, were computed. For this special case solutions have already been found by Lessen *et al.* (1968). Thus it was possible to check our computer programs by comparison of the results with those of Lessen *et al.* For example, they

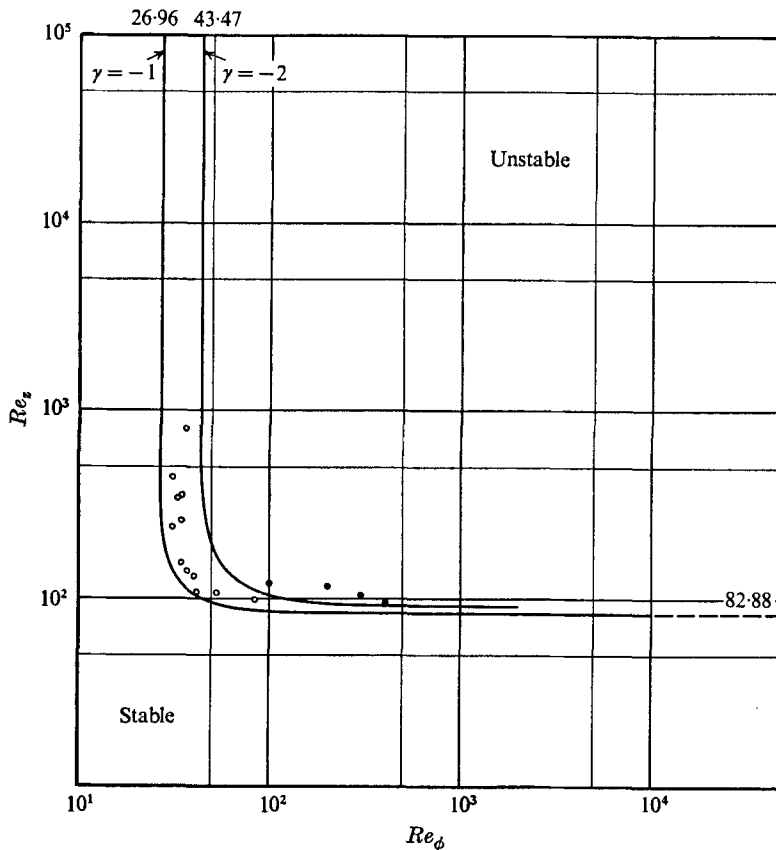


FIGURE 3. Stability boundaries at  $\gamma = -1$  and  $\gamma = -2$  and experimental results.  $\circ$ , observation of disturbance vortices;  $\bullet$ , drag measurements.

found, at  $Re_z = 200$  and  $\bar{\alpha} = \gamma = 1$ ,

$$c = 0.645 - 0.129i;$$

the author's result is

$$c = 0.64526 - 0.12921i.$$

As a next step the eigenvalues were calculated starting from  $Re_\phi = 0$  and proceeding with  $Re_z = \text{constant}$  to increasingly higher azimuthal Reynolds numbers  $Re_\phi$ . Guided by the results obtained previously by Ludwig (1960, 1961), Wedemeyer (1969) and Hung *et al.* (1972) for the stability of helical flow in a small annulus, by Pedley (1969, appendix) for a rapidly rotating pipe and by Lessen & Paillet (1974) for an unbounded swirling jet, we assumed that disturbances in the pipe would be found only for *negative* azimuthal wavenumbers  $\gamma$ . (See also §4 below.) Accordingly neutral curves (curves on which  $\text{Im}(c)$  vanishes) were obtained for various  $\bar{\alpha}$  (figure 2*a*) and various negative  $\gamma$  (figure 2*b*). The envelope of all these curves represents the overall stability boundary, on the assumption that all relevant modes have been considered. For larger axial and azimuthal Reynolds numbers this stability boundary was determined in two steps: in the first step the most unstable mode for fixed  $\gamma$  was evaluated as a function of  $\bar{\alpha}$  and

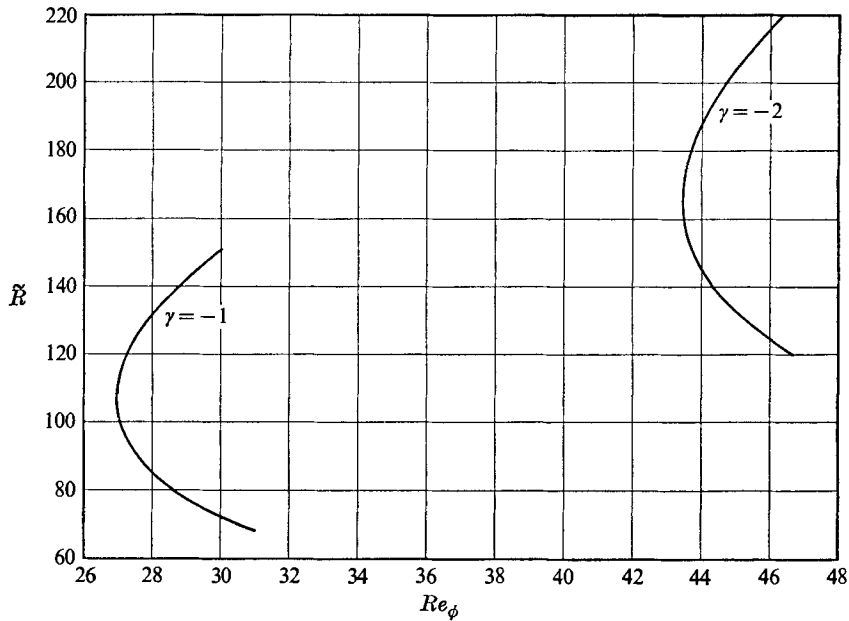


FIGURE 4. Neutral curves in the case  $Re_z \rightarrow \infty$  at  $\gamma = -1$  and  $\gamma = -2$ .

in the second step the point  $(Re_\phi, Re_z)$  for which  $\text{Im}(c)$  vanishes was determined. In this way the neutral curves were calculated up to  $Re_z = 100\,000$  for  $\gamma = -1$  and  $\gamma = -2$  (figure 3), up to  $Re_\phi = 10\,000$  for  $\gamma = -1$  and up to  $Re_\phi = 2000$  for  $\gamma = -2$ .

3.2. Infinite axial Reynolds number

The solution of (2.9)–(2.12) shows that, for sufficiently large axial Reynolds numbers ( $Re_z \geq 4000$ ), the product  $\tilde{R} = \bar{\alpha} Re_z$  remains constant on the neutral curve ( $\tilde{R} = 106.6$  for  $\gamma = -1$  and  $\tilde{R} = 165.4$  for  $\gamma = -2$ ; see figure 1) and the eigenvalue  $c$  is independent of  $Re_z$ . Thus this eigenvalue is a suitable starting value for the numerical solution of (2.15)–(2.18), which was achieved in a similar manner to that described in §3.1. Figure 4 shows the curves  $\tilde{R}$  vs.  $Re_\phi$  on which  $\text{Im}(c)$  vanishes for  $\gamma = -1$  and  $\gamma = -2$ .

4. Results and discussion

The results of the calculations show that unstable modes do indeed exist if a finite rigid rotation is superimposed on Hagen–Poiseuille flow. From figures 2(b) and 3 it is apparent that the most unstable disturbances are those with  $\gamma = -1$ . At  $\gamma = -1$  there exists one neutral curve for each axial wavenumber  $\bar{\alpha}$  (figure 2a). The envelope of all these curves, the overall neutral curve, matches for sufficiently high azimuthal Reynolds numbers ( $Re_\phi \geq 4000$ ) the line

$$Re_z = 82.88,$$

which is exactly the value found by Pedley (1969) and Joseph & Carmi (1969) in the case  $Re_\phi \rightarrow \infty$ . As the axial Reynolds number  $Re_z$  tends to infinity, the stability

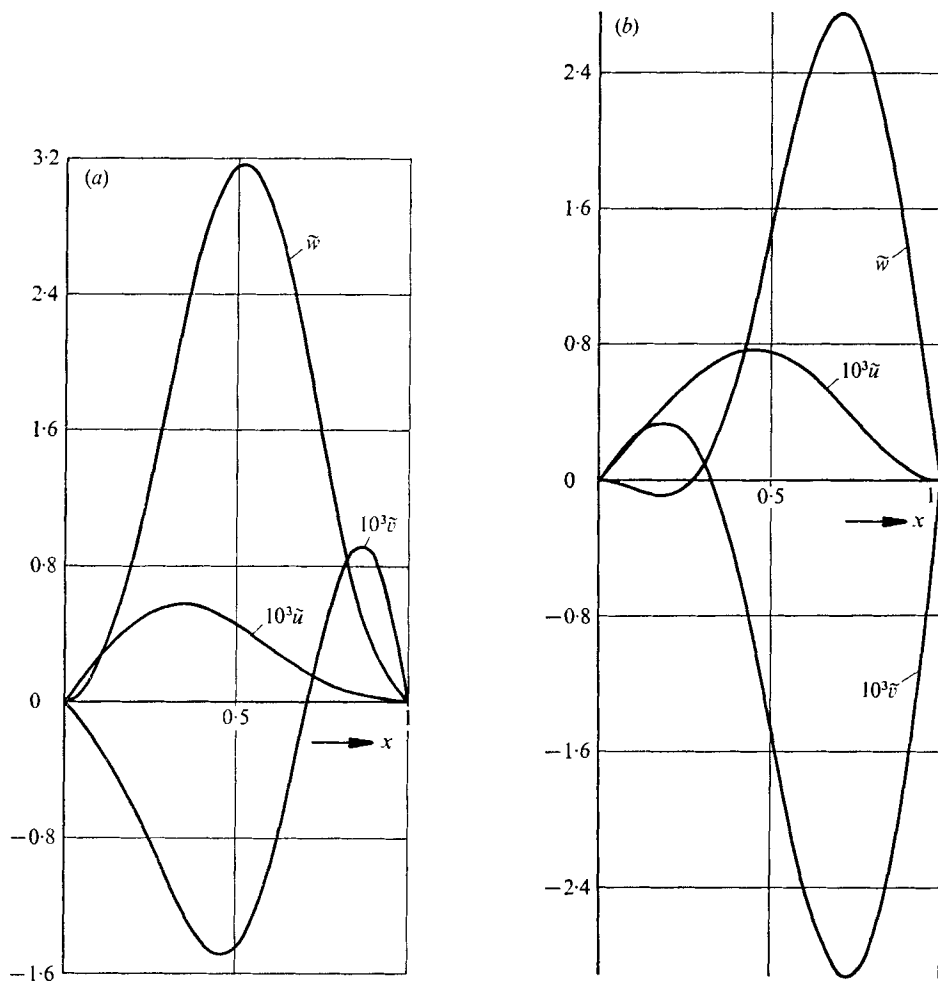


FIGURE 5. (a) Real and (b) imaginary parts of typical eigenfunctions at  $Re_z = 100\,000$  and  $Re_\phi = 27$  with  $\bar{\alpha} = 0.001075$  and  $\gamma = -1$ .

boundary seems to approach an analogous limiting value. The solution of the differential equations (2.15)–(2.18) shows (figure 4) that these limiting values are

$$Re_\phi = 26.96 \quad \text{at} \quad \tilde{R} = 106.6 \quad \text{for} \quad \gamma = -1$$

and

$$Re_\phi = 43.47 \quad \text{at} \quad \tilde{R} = 165.4 \quad \text{for} \quad \gamma = -2.$$

The existence of the finite  $Re_\phi$  values is consistent with the accepted view that Hagen–Poiseuille flow ( $Re_\phi \equiv 0$ ) is linearly stable against small three-dimensional disturbances at all axial Reynolds numbers. An example of typical unstable eigenfunctions (at  $Re_z = 100\,000$  and  $Re_\phi = 27$ ) is shown in figures 5(a) and (b).

Furthermore the above results tend to support the conjecture, made in §1 above, that linear instability may, nevertheless, play an initial role in experiments on the transition to turbulence of HPF at very high (axial) Reynolds



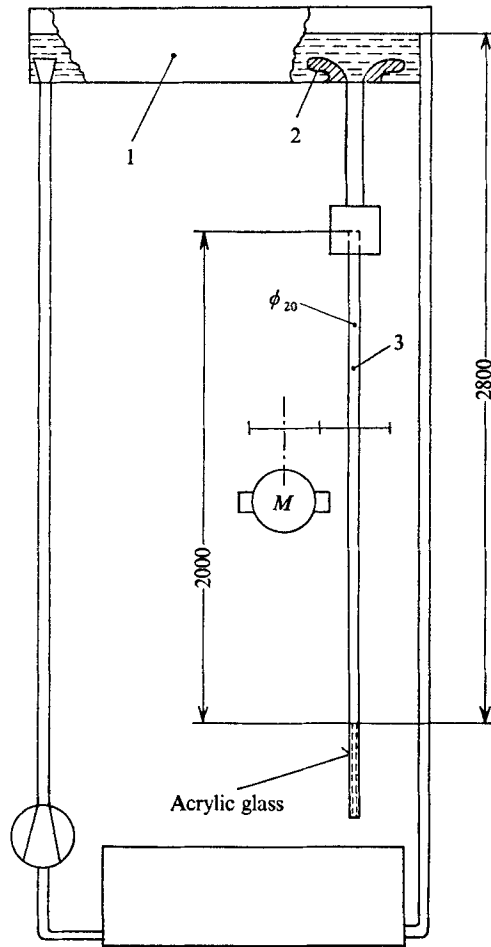


FIGURE 6. Schematic diagram of experimental set-up (dimensions in mm).

numbers. Although the present results cannot be applied quantitatively, it appears from an argument due to McIntyre (see Pedley 1969, appendix) that the physical mechanism of the instability is likely to be insensitive to the precise form of the axial and azimuthal velocity profiles, as long as there is some axial shear and some rotation. (This is in contrast to classical shear instabilities, and is because the present instabilities are physically more like Taylor vortices, when viewed in an appropriate co-ordinate system. The argument suggests, incidentally, why negative values of  $\gamma$  should dominate the instability properties as soon as there is some rotation.)

It should of course be realized that, although the neutral curves give sufficient conditions for the onset of instabilities, they need not correspond to the transition to turbulence. At low  $Re_z$  the amplification rate of the unstable disturbances is low and their increase with growing  $Re_z$  would probably lead to another stable flow (again by analogy to Taylor vortices) rather than to turbulence. Only at very high Reynolds numbers may the neutral curve and the transition boundary be

expected to coincide. And, indeed, findings of experimenters seem to point in this direction. Bhat (1966) maintained laminar flow up to  $Re_z = 40\,000$ . At this axial Reynolds number a superimposed rotational velocity with an azimuthal Reynolds number of about 27 would be sufficient to initiate instability. Obviously such an extremely small azimuthal velocity, involving streamline directions only  $0.04^\circ$  off axial, could well remain undetected unless one were to look for it.

### 5. Comparison of the calculated neutral curve with experiment

In order to check the results of the numerical calculations a few simple experiments were performed. The apparatus used is shown in figure 6. The fluid flows from the tank (1) through a properly finished inlet (2) into a pipe (3) which is being rotated by means of an adjustable-speed electric motor ( $M$ ). After a certain distance from the inlet the fluid rotates rigidly with the pipe.

It was shown by Christiansen & Lemmon (1965) and Sparrow, Lin & Lundgren (1964) that HPF is fully developed after a running length  $l$  given by

$$l/R = 0.113Re_z. \quad (5.1)$$

The development of the rigid rotation follows essentially the same law as that of HPF (at least for  $Re_z \gtrsim Re_\phi$ ; cf. Pedley 1969, equation (6.5)), so we can expect the basic flow to be fully developed after the length  $l$ . Thus, for  $Re_z < 400$  and  $Re_\phi < 400$  the basic flow is established after about one quarter of the pipe length (see figure 6). The fluid was glycerine because of the ease of adjusting its viscosity by heating or cooling. With the viscosity constant (that is, at constant axial Reynolds number  $Re_z$ ), the spin rate of the pipe (and thus the azimuthal Reynolds number  $Re_\phi$ ) was gradually increased until the first disturbance vortices appeared in the glass part immediately upstream of the pipe orifice (figure 6), or, conversely,  $Re_\phi$  was decreased until the vortices disappeared. (In this part of the pipe disturbances from the inlet cannot be expected as was shown by Tatsumi 1952.) The first appearance of disturbances was interpreted as the onset of instability. The results of these experiments are depicted in figure 3 as small circles. The agreement with the theoretical curve for  $\gamma = -1$  is quite good. To confirm the right branch of the curve the method described above was not applicable because the axial Reynolds number  $Re_z$  could be varied only by altering the viscosity of the fluid. This causes some variation in the azimuthal Reynolds number  $Re_\phi$  too. Therefore the transition from stable to unstable flow was slow and observation of the occurrence of disturbance vortices did not yield reproducible data. For this reason an attempt was made to confirm the results by measuring the flow drag in the pipe. The drag must increase on the occurrence of instabilities. The results show a little more scatter, probably because this method is less sensitive.

A further verification of the stability boundary is obtained by observation of the spiral angles of the disturbance vortices. The spiral angle  $\Psi$  at the wall is given by

$$\cot \Psi = \frac{1}{R} \frac{dz}{d\phi} = -\frac{\gamma}{\alpha}. \quad (5.2)$$

At  $Re_z = 200$  the most unstable mode has axial wavenumber  $\bar{\alpha} = 0.5$  (and  $\gamma = -1$ ). This leads to

$$\cot \Psi = 2. \quad (5.3)$$

The spiral angles observed in the unstable flow at  $Re_z = 200$  and  $Re_\phi \approx 70$  range from  $\cot \Psi = 1.92$  to  $\cot \Psi = 2.2$ , which agrees very well with the theoretical value.

## REFERENCES

- BHAT, W. V. 1966 Ph.D. dissertation, University of Rochester, New York.
- CHRISTIANSEN, E. B. & LEMMON, H. E. 1965 Entrance region flow. *A.I.Ch.E. J.* **11**, 995.
- CROWDER, H. J. & DALTON, C. 1971 Stability of Poiseuille flow in a pipe. *J. Comp. Phys.* **7**, 12.
- DAVEY, A. & DRAZIN, P. G. 1969 The stability of Poiseuille flow in a pipe. *J. Fluid Mech.* **36**, 209.
- GILL, A. E. 1973 Least damped disturbance to Poiseuille flow in a circular pipe. *J. Fluid Mech.* **61**, 97.
- HUNG, W. L., JOSEPH, D. D. & MUNSON, B. R. 1972 Global stability of spiral flow. Part 2. *J. Fluid Mech.* **51**, 593.
- JOSEPH, D. D. & CARMÍ, S. 1969 Stability of Poiseuille flow in pipes, annuli and channels. *Quart. Appl. Math.* **26**, 575.
- KIESSLING, I. 1963 Über das Taylorsche Stabilitätsproblem bei zusätzlicher axialer Durchströmung der Zylinder. *D.V.L. Rep.* no. 290.
- LEITE, R. J. 1959 An experimental investigation of the stability of Poiseuille flow. *J. Fluid Mech.* **5**, 81.
- LESSEN, M. & PAILLET, F. 1974 The stability of a trailing line vortex. Part 2. Viscous theory. *J. Fluid Mech.* **65**, 769.
- LESSEN, M., SADLER, S. & LIU, T. Y. 1968 Stability of pipe Poiseuille flow. *Phys. Fluids*, **11**, 1404.
- LUDWIG, H. 1960 Stabilität der Strömung in einem zylindrischen Ringraum. *Z. Flugwiss.* **8**, 135.
- LUDWIG, H. 1961 Ergänzung zu der Arbeit "Stabilität der Strömung in einem zylindrischen Ringraum". *Z. Flugwiss.* **9**, 359.
- LUDWIG, H. 1964 Experimentelle Nachprüfung der Stabilitätstheorien für reibungsfreie Strömungen mit schraubenförmigen Stromlinien. *Z. Flugwiss.* **12**, 304.
- MACKRODT, P.-A. 1967 Spiralströmungen im zylindrischen Ringraum hinter Leitradern. *Z. Flugwiss.* **15**, 335.
- MACKRODT, P.-A. 1971 Stabilität von Hagen-Poiseuille-Strömungen mit überlagerter starrer Rotation. *Rep. MPI Ström. Forsch. u. Aerodyn. Vers. Anst., Göttingen*, no. 55.
- MACKRODT, P.-A. 1973 Stabilität der Hagen-Poiseuille-Strömung mit überlagerter starrer Rotation bei sehr hohen Reynoldszahlen. *DFVLR-AVA, Göttingen Rep.* no. 251 73 A 25.
- METCALFE, R. W. & ORSZAG, S. A. 1973 Numerical calculation of the linear stability of pipe flows. *Bull. Am. Phys. Sci.* **18**, 11.
- MOTT, J. E. & JOSEPH, D. D. 1968 Stability of parallel flow between concentric cylinders. *Phys. Fluids*, **11**, 2065.
- NAGIB, H. M., LAVAN, Z., FEJER, A. A. & WOLF, L. 1971 Stability of pipe-flow with superposed solid body rotation. *Phys. Fluids*, **14**, 766.
- PEDLEY, T. J. 1968 On the instability of rapidly rotating shear flows to non-axisymmetric disturbances. *J. Fluid Mech.* **31**, 603.
- PEDLEY, T. J. 1969 On the instability of viscous flow in a rapidly rotating pipe. *J. Fluid Mech.* **35**, 97.
- RESHOTKO, E. 1958 Experimental study of the stability of pipe flow. I. Establishment of an axially symmetric Poiseuille flow. *Jet Propulsion Lab., Caltech Prog. Rep.* no. 20-364.

- REYNOLDS, O. 1883 An experimental investigation of the circumstances which determine whether the motion of water shall be direct or sinuous and of the law of resistance in parallel channels. *Phil. Trans. A* **174**, 935. (See also *Papers on Mechanical and Physical Subjects*, vol. 2, p. 51. Cambridge University Press.)
- REYNOLDS, O. 1895 On the dynamical theory of incompressible viscous fluids and the determination of the criterion. *Phil. Trans. A* **186**, 123. (See also *Papers on Mechanical and Physical Subjects*, vol. 2, p. 535. Cambridge University Press.)
- SALWEN, H. & GROSCHE, C. E. 1972 Stability of Poiseuille flow in a pipe of circular cross-section. *J. Fluid Mech.* **54**, 93.
- SCHILLER, L. 1922 Untersuchungen über laminare und turbulente Strömung. *Forsch. Geb. Ing. Wes. H.* no. 248.
- SEXL, TH. 1927a Stabilitätsfragen der Poiseuilleschen und Couetteschen Strömung. *Ann. Phys. (Leipzig)*, **83**, 835.
- SEXL, TH. 1927b Über dreidimensionale Störungen der Poiseuilleschen Strömung. *Ann. Phys. (Leipzig)*, **84**, 807.
- SPARROW, E. M., LIN, S. H. & LUNDGREN, T. S. 1964 Flow development in the hydrodynamic entrance region of tubes and ducts. *Phys. Fluids*, **7**, 338.
- STROHL, J. 1969 Hydrodynamic stability of Poiseuille flow in a rotating pipe. M.Sc. thesis, Illinois Institute of Technology, Chicago.
- TATSUMI, T. 1952 Stability of the laminar inlet-flow prior to the formation of Poiseuille régime. *J. Phys. Soc. Japan*, **7**, 489, 495.
- WEDEMEYER, E. 1967 Einfluss der Zähigkeit auf die Stabilität der Strömung in einem schmalen Ringraum mit zusätzlichem axialem Durchfluss. *AVA Rep. Göttingen*, no. 67 A 34.
- WEDEMEYER, E. 1969 Stabilität spiraliger Strömungen in einem zylindrischen Ringraum. *Rep. MPI Ström. Forsch. u. Aerodyn. Vers. Anst., Göttingen*, no. 44.